

Supplement to 'Ozone source attribution in polluted European areas during summer as simulated with MECO(n)'

Markus Kilian, Volker Grewe, Patrick Jöckel, Astrid Kerkweg, Mariano Mertens,
Andreas Zahn, Helmut Ziereis

Institut für Physik der Atmosphäre, DLR Oberpfaffenhofen

01.03.2023

1 Total emissions

emission sector	Global	EU	NA	EA	ROW
Land transport	21.7	2.6 (0.7)	4.3 (1.1)	4.5 (1.1)	10.3 (2.5)
Non-traffic	43.5	3.9 (1.1)	5.2 (1.3)	14.9 (3.6)	19.5 (4.7)
Shipping	19.3				
Bioburn + AWB	8.2				
Biogenic	13.0				
Lightning	12.1				

Table S1. Totals of NO_x emissions (in $\text{Tg}(\text{NO}) \text{ a}^{-1}$) for our tagging regions: globally, in Europe (EU), in North America (NA), in East Asia (EA) and in the rest of the world (ROW) for 2017 and JJA 2017 in brackets. Source attribution for our tagging regions is only applied for the land transport and anthropogenic non-traffic sector.

2 Definition of NO_y

For the comparison between the aircraft in situ measurements and the model results we use the following definition of NO_y :

$$\begin{aligned} \text{NO}_y = & N + \text{NO}_2 + \text{NO} + \text{HNO}_3 + \text{HNO}_4 \\ 5 & + \text{HONO} + 2x\text{N}_2\text{O}_5 + \text{PAN} + \text{HNO} + \text{ISON} \\ & + \text{LC}_4\text{H}_9\text{NO}_3 + \text{IC}_3\text{H}_7\text{NO}_3 \\ & + \text{BrNO}_2 + \text{BrNO}_3 + \text{ClNO}_2 \\ & + \text{ClNO}_3 \end{aligned}$$

Please note, that the definition of NO_y family used by the TAGGING method differs slightly, because PAN is tagged individually due to the large importance of PAN for long range transport (see Grewe et al., 2017).

3 Online flagging of emissions

To subdivide the global emission files which are used as input of the model into regional parts corresponding to the individual regions we applied the SCALC (Simple CALCulations) submodel. Kern (2013) describes the submodel in detail, which allows the multiplication of two channel objects, here applied in order to prepare the emissions for the tagging by the source regions (see Appendix C in Kern, 2013). The anthropogenic emission inventory EDGAR is multiplied with a flag file containing 1 for each tagging region and 0 everywhere else. This generates new emission channel objects, where emissions are enabled in the tagged region and set to zero everywhere else. For the present study the simple multiplication has been further developed to ensure that all emissions, also along coastlines, are conserved.

4 Pre-processing of EDGAR

During the preparation of the EDGAR emissions the different sectors from EDGAR are mapped on a simplified sector definition containing the sectors anthropogenic non-traffic, land transport and shipping. During the summation of the sector each sub-sector of EDGAR is vertically distributed according to Mailler et al. (2013). Table S2 shows the vertical disaggregation for each level and each emission sector. In the pre-processing the distribution onto 7 levels was applied, by multiplying the scalar at each grid point (emission) with a vector containing each particular fraction (Table S2).

SNAP sectors ¹										
Level [m]	1	2	3	4	5	6	7	8	9	10
0	0.	11.	0.	20.	20.	100	100	100	2.	100
20	0.	89.	21.3	70.	70.	0.	0.	0.	8.	0.
92	0.25	0.	75.4	7.	6.	0.	0.	37.	0.	0.
184	51.	0.	3.3	1.	3.	0.	0.	51.	0.	0.
324	45.3	0.	0.	0.	0.	0.	0.	2.	0.	0.
522	3.29	0.	0.	0.	0.	0.	0.	0.	0.	0.
781	0.2	0.	0.	0.	0.	0.	0.	0.	0.	0.

Table S2. Vertical disaggregation fractions (%) per European Monitoring and Evaluation Programme (EMEP) levels in m (left column) and per SNAP sectors from Bieser et al. (2011), with additional 0–20 m layer for surface emissions (adapted from, Mailler et al., 2013).

¹SNAP sectors: 1. combustion in energy and transformation industry, 2. non-industry combustion, 3. comb. in manufacturing industry, 4. prod. processes, 5. extraction of fossil fuels, 6. solvent use, 7. road transport, 8. other mobile sources, 9. waste treatment, 10. agriculture, 11. other sources and sinks.

5 Pre-processing of GFAS

The biomass burning emissions in our simulations are prescribed by the GFAS data set from the ECMWF CAMS. In order to represent the dispersion of biomass burning emissions by the pyro-convection in an appropriate way, in the pre-processing the GFAS emissions are vertically distributed onto 6 levels up to 4500 m depending on their geographical location (Dentener

5 et al., 2006, see Table S3).

Level [m]*							
Region	50	300	750	1500	2500	4500	
tropical (30 S-30 N)	20.	40.	40.	0.	0.	0	
Temperate (30 N-60 N, 30 S-60 S)	20.	20.	20.	40.	0.	0	
Boreal (Eurasia)	10.	10.	20.	20.	40.	0	
Boreal (Canada)	10.	10.	10.	10.	20.	40	

Table S3. Fractional distribution (in %) of emission heights for wild-land fires (Dentener et al., 2006, from). * contributions assigned to heights below the actual surface altitude are moved into the lowest applicable height range and contribution of the 0-100m altitude are always emitted in the lowest model layer.

6 Additional figures

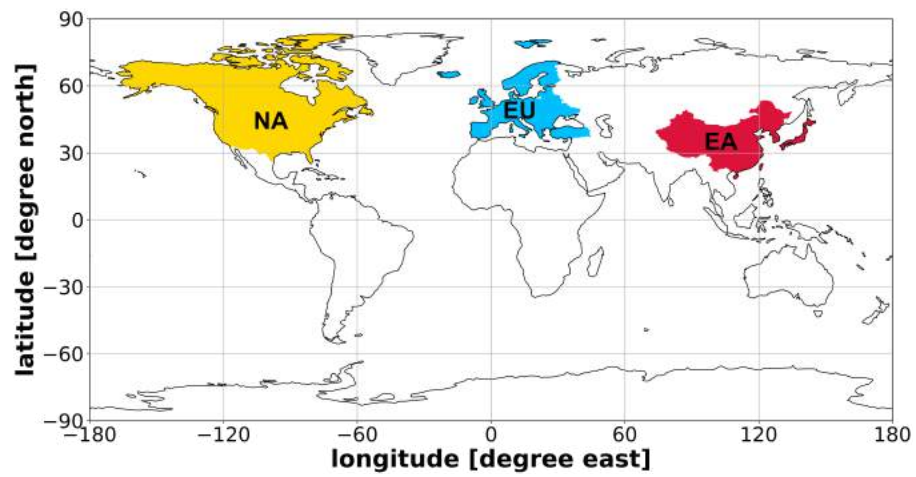


Figure S1. Source regions (marked by color) for tagging in our MECO(2) model setup are defined as: North America (NA), Europe (EU) and East Asia (EA). All other countries and the ocean are considered as rest of the world (ROW).

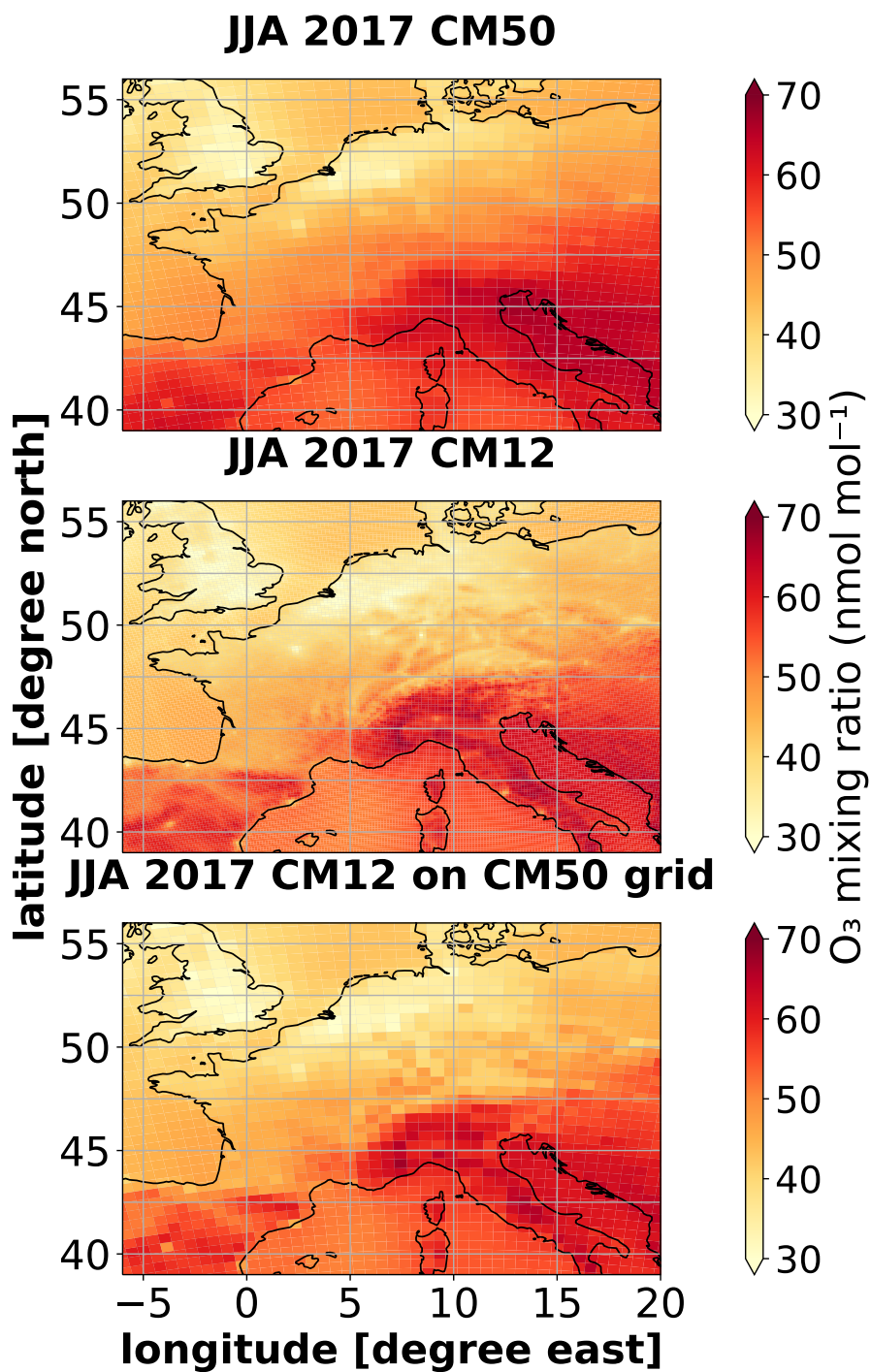


Figure S2. Comparison of ground-level ozone for JJA 2017 between CM50 (50 km) and CM12 (12 km).

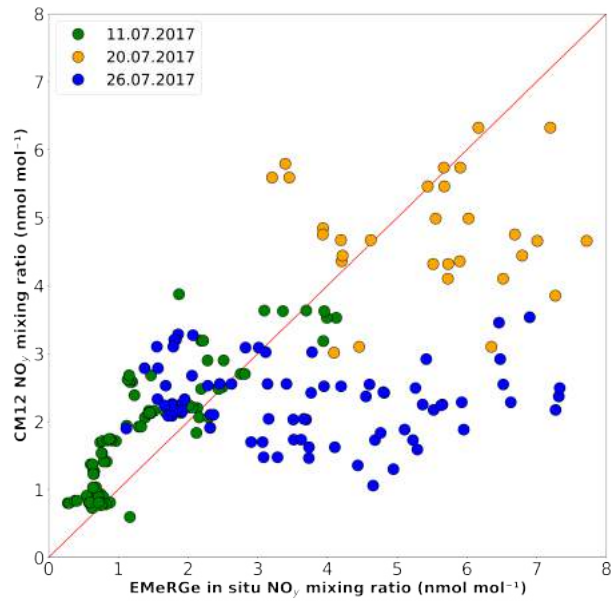


Figure S3. Comparison of the NO_y mixing ratios in nmol mol^{-1} between the CM12 model results (y-axis) and the HALO in situ measurements on the x-axis for all three flight dates 11.07.2017, 20.07.2017 and 26.07.2017.

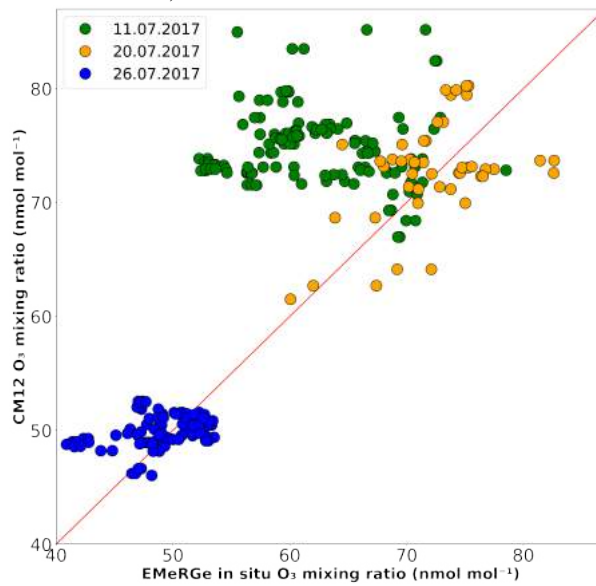


Figure S4. Comparison of the O_3 mixing ratios in nmol mol^{-1} between the CM12 model results (y-axis) and the HALO in situ measurements on the x-axis for all three flight dates 11.07.2017, 20.07.2017 and 26.07.2017.

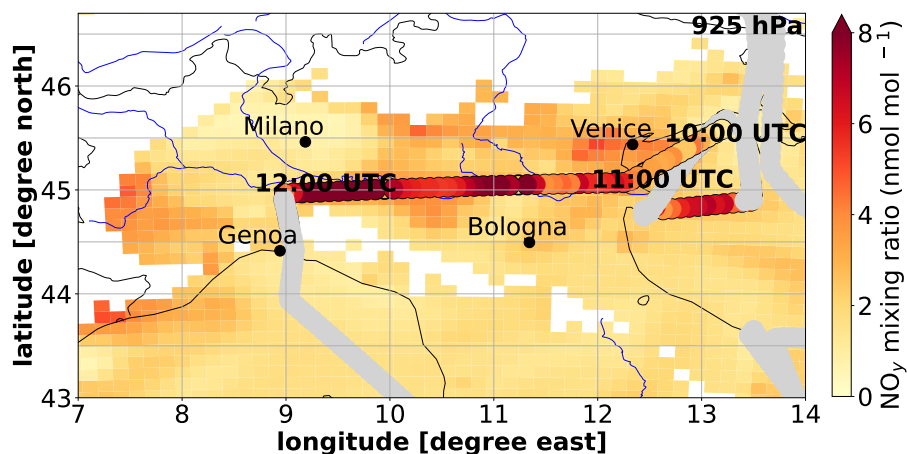


Figure S5. NO_y mixing ratios in nmol mol^{-1} at 12 UTC of the model output of CM12 (background color) at 925 hPa and the HALO in situ measurements (filled circles) for the flight date 20.07.2017 in Po Valley. The grey filled circles mask the measurement data, where HALO flew above or below the shown pressure level.

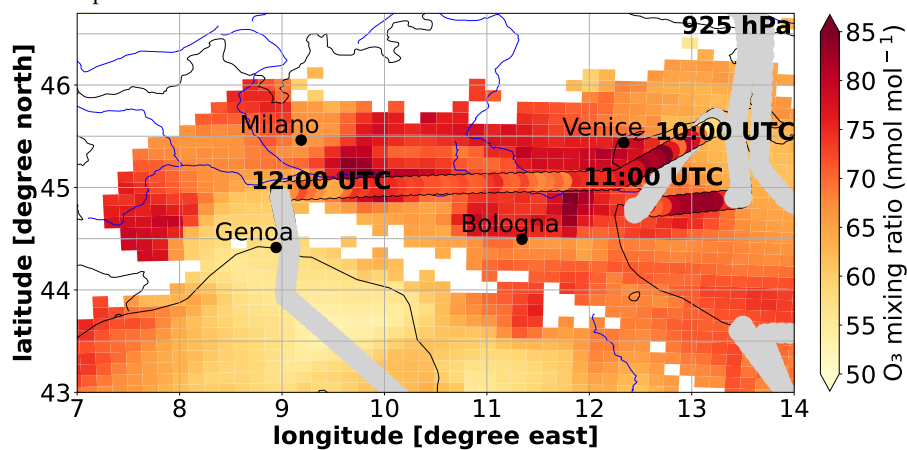


Figure S6. O_3 mixing ratios in nmol mol^{-1} at 12 UTC of the model output of CM12 (background color) at 925 hPa and the HALO in situ measurements (filled circles) for the flight date 20.07.2017 in Po Valley. The grey filled circles mask the measurement data, where HALO flew above or below the shown pressure level.

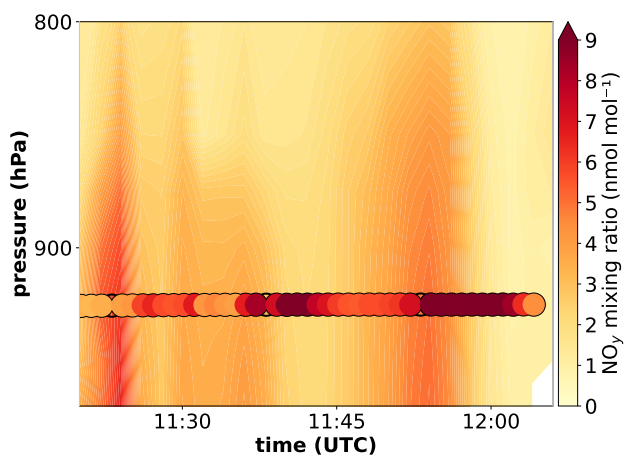


Figure S7. Comparison between CM12 model results of NO_y mixing ratios in nmol mol^{-1} sampled along flight path of HALO (background color) with the HALO in situ measurements (filled circles) for the flight date 20.07.2017 in the Po Valley.

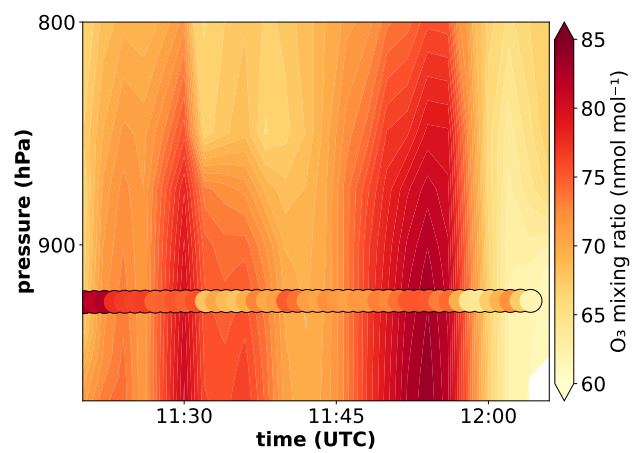


Figure S8. Comparison between CM12 model results of O_3 mixing ratios in nmol mol^{-1} sampled along flight path of HALO (background color) with the HALO in situ measurements (filled circles) for the flight date 20.07.2017 in the Po Valley.

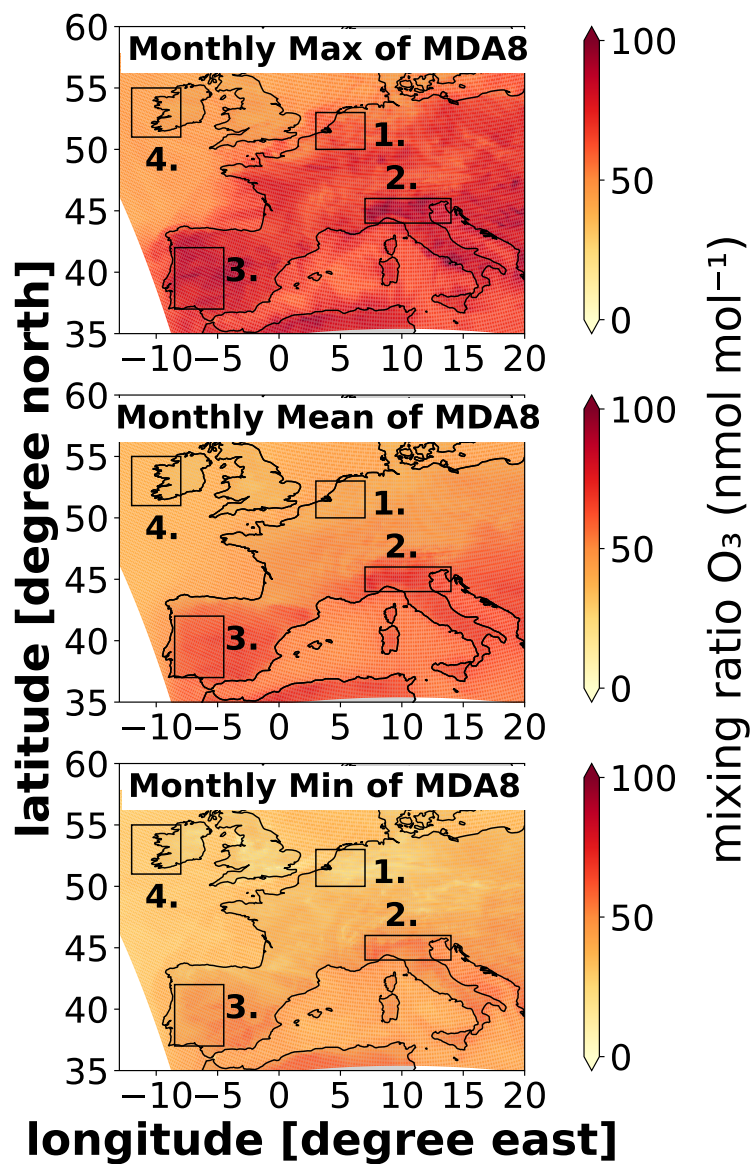


Figure S9. Shown is ozone in July 2017 during the monthly maximum of the maximum daily 8-h average (MDA8), the monthly mean of MDA8 and the monthly minimum of MDA8 as mixing ratios in nmol mol^{-1} based on 1-hourly model output from CM12. The black rectangles mark the study areas with 1. Benelux, 2. Po Valley, 3. Spain and 4. West Ireland.

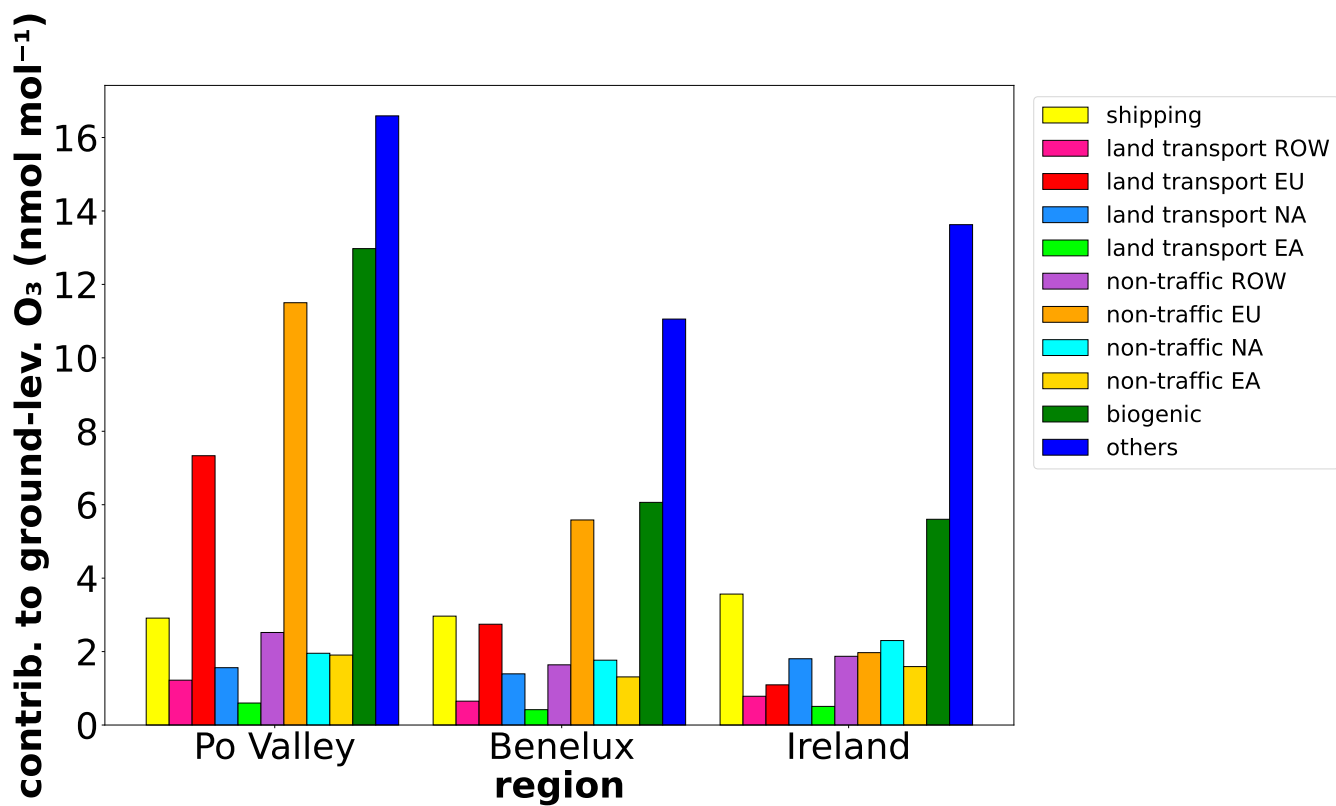


Figure S10. Monthly mean absolute contribution of different emission sectors and regions to ground-level ozone in the three regions Benelux, Po Valley, and West Ireland for JJA 2017 as simulated with CM12.

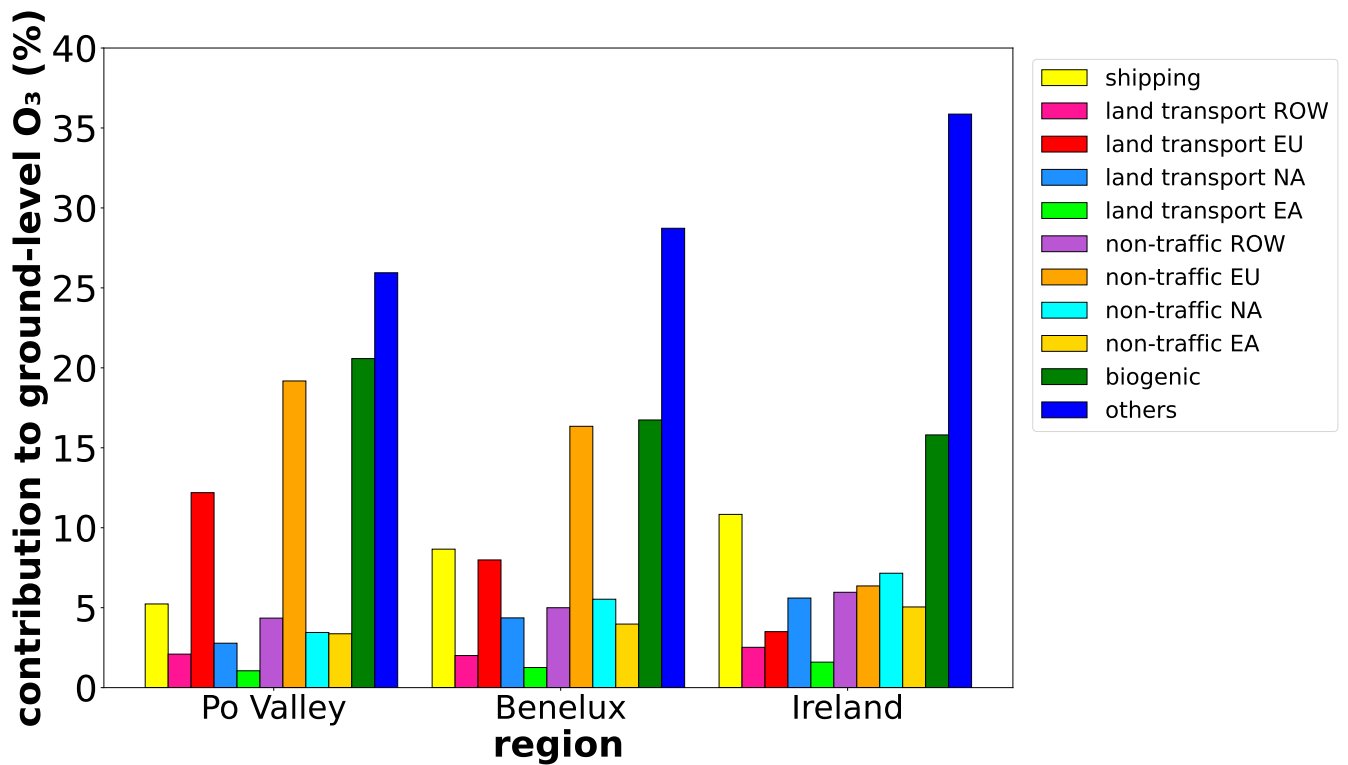


Figure S11. Monthly mean relative contribution of different emission sectors and regions to ground-level ozone in the three regions Benelux, Po Valley, and West Ireland for JJA 2017 as simulated with CM12.

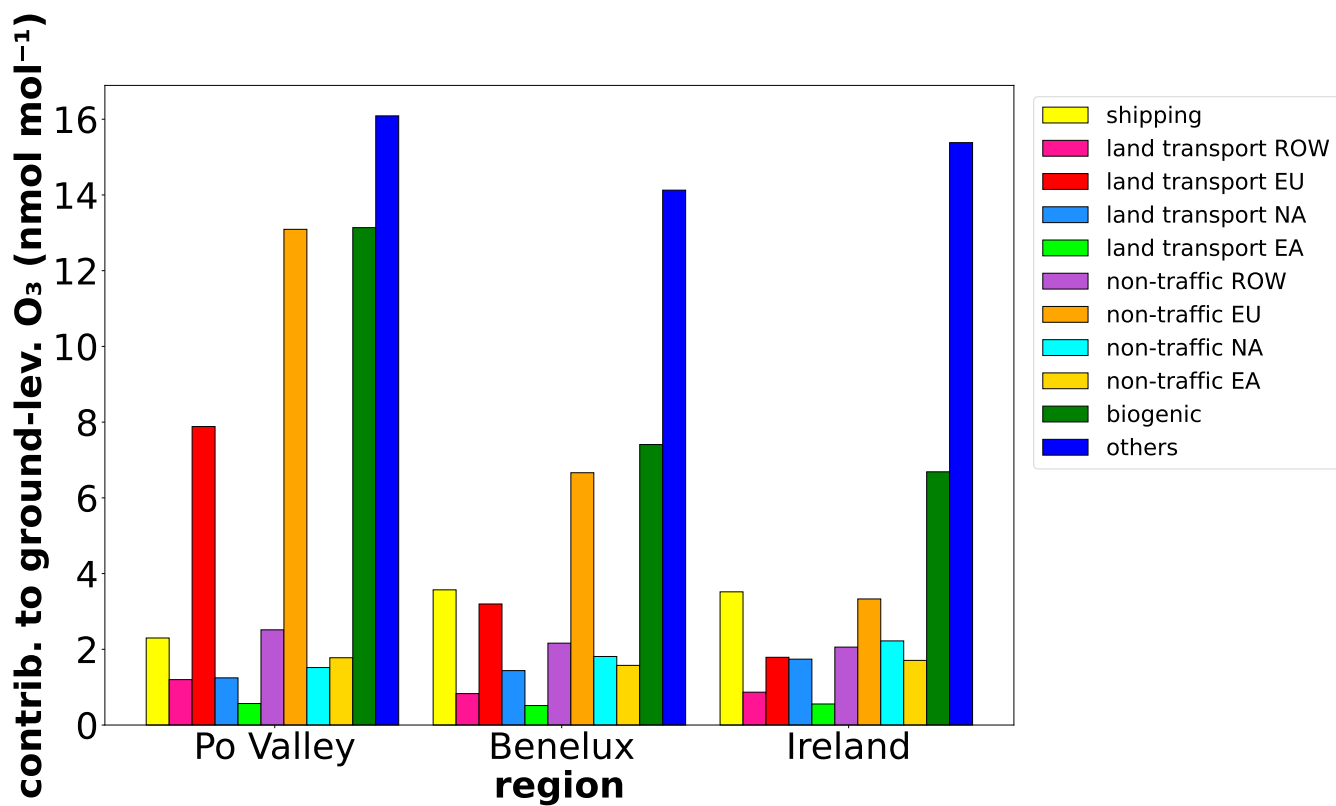


Figure S12. Monthly mean absolute contribution of different emission sectors and regions to ground-level ozone in the three regions Benelux, Po Valley, and West Ireland for JJA 2018 as simulated with CM12.

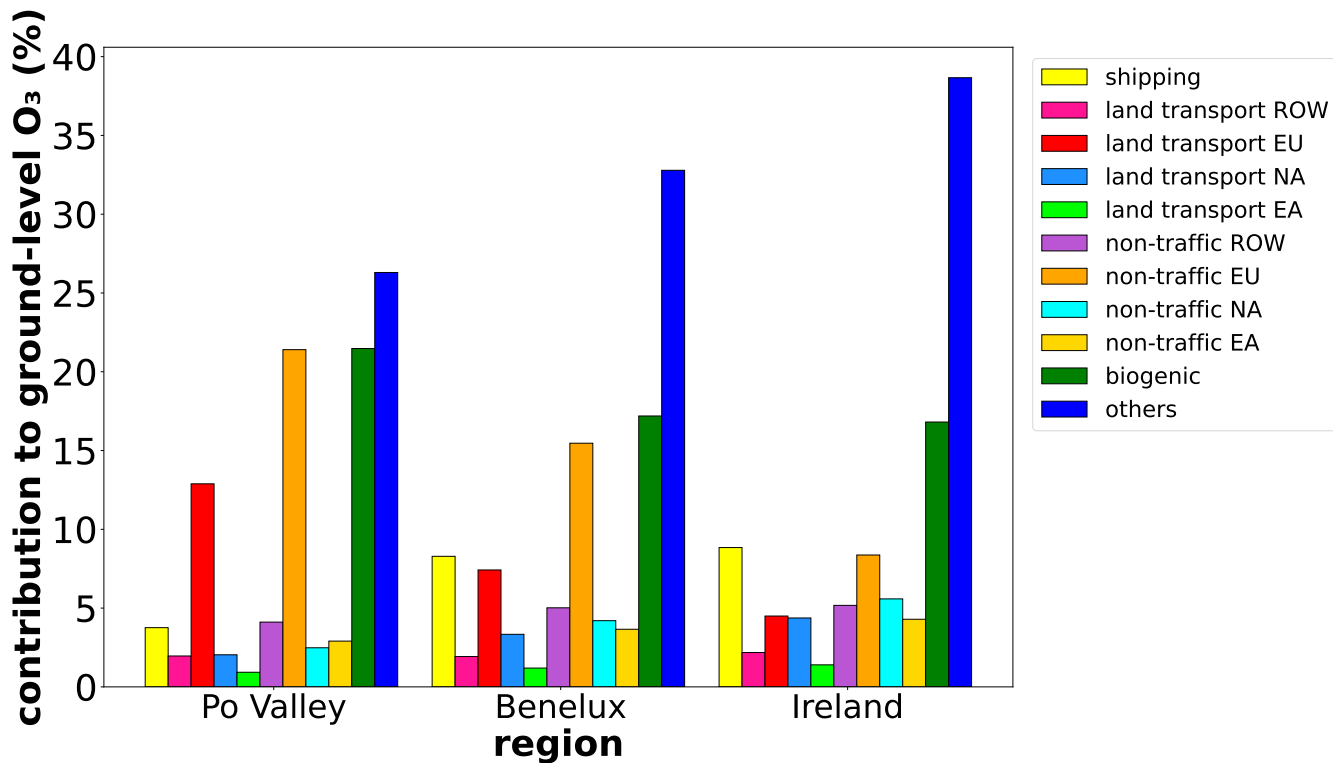


Figure S13. Monthly mean relative contribution of different emission sectors and regions to ground-level ozone in the three regions Benelux, Po Valley, and West Ireland for JJA 2018 as simulated with CM12.

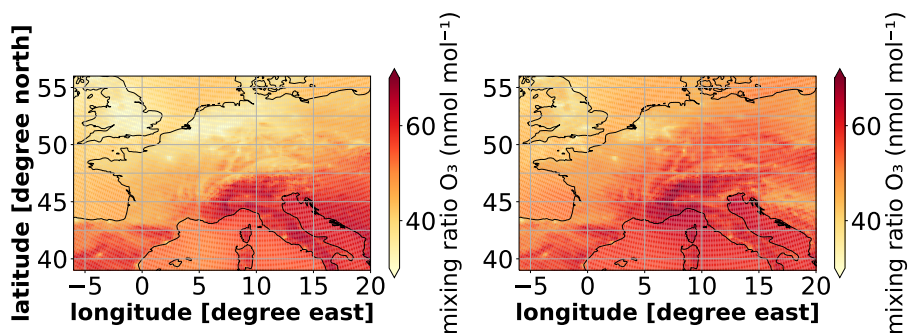


Figure S14. Comparison of JJA ground-level ozone in CM12 between the years 2017 and 2018.

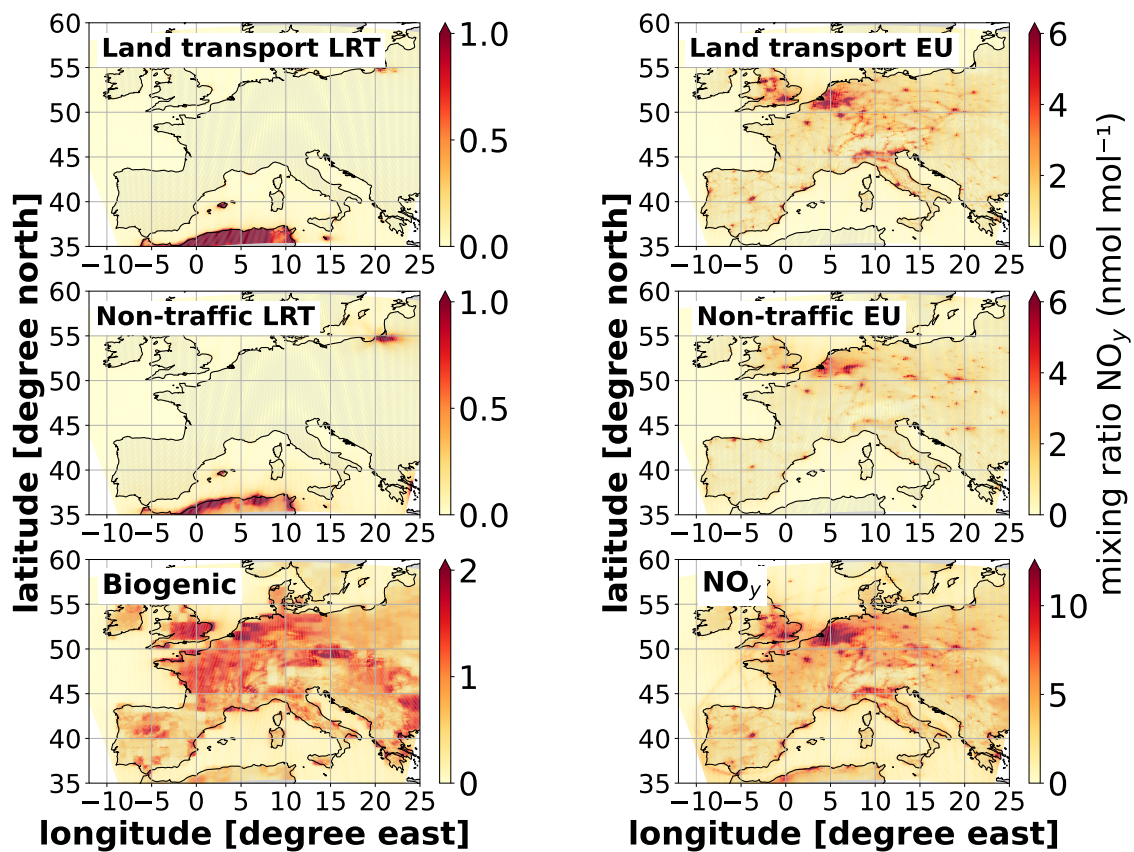


Figure S15. Monthly mean absolute contributions of NO_y as mixing ratios in nmol mol^{-1} for JJA 2017 from long-range transported (LRT: ROW + NA + EA) NO_y , biogenic emissions (for NO_y soil- NO_x), and European emissions by sectors and total NO_y (lower right) as simulated with CM12.

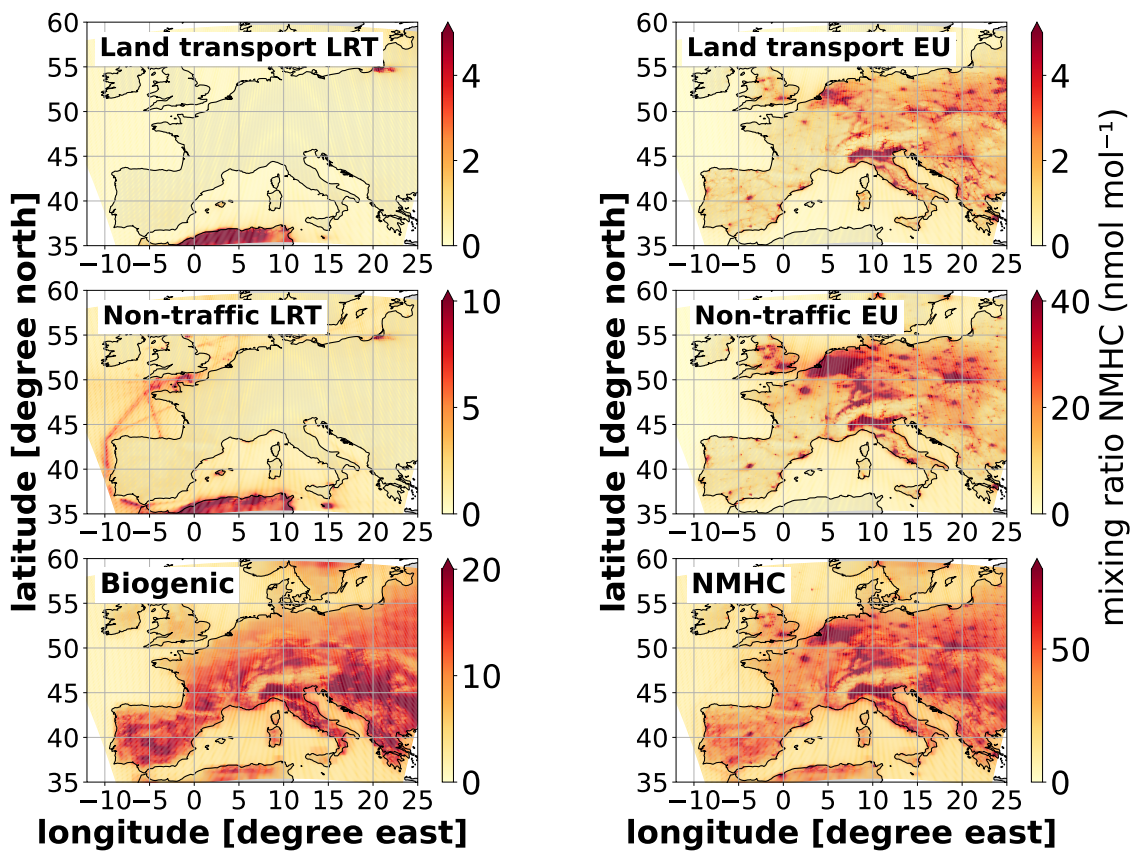


Figure S16. Monthly mean absolute contributions of NMHC as mixing ratios in nmol mol^{-1} for JJA 2017 from long-range transported (LRT: ROW + NA + EA) NMHC, biogenic, and European emissions by sectors and total NMHC (lower right) as simulated with CM12.

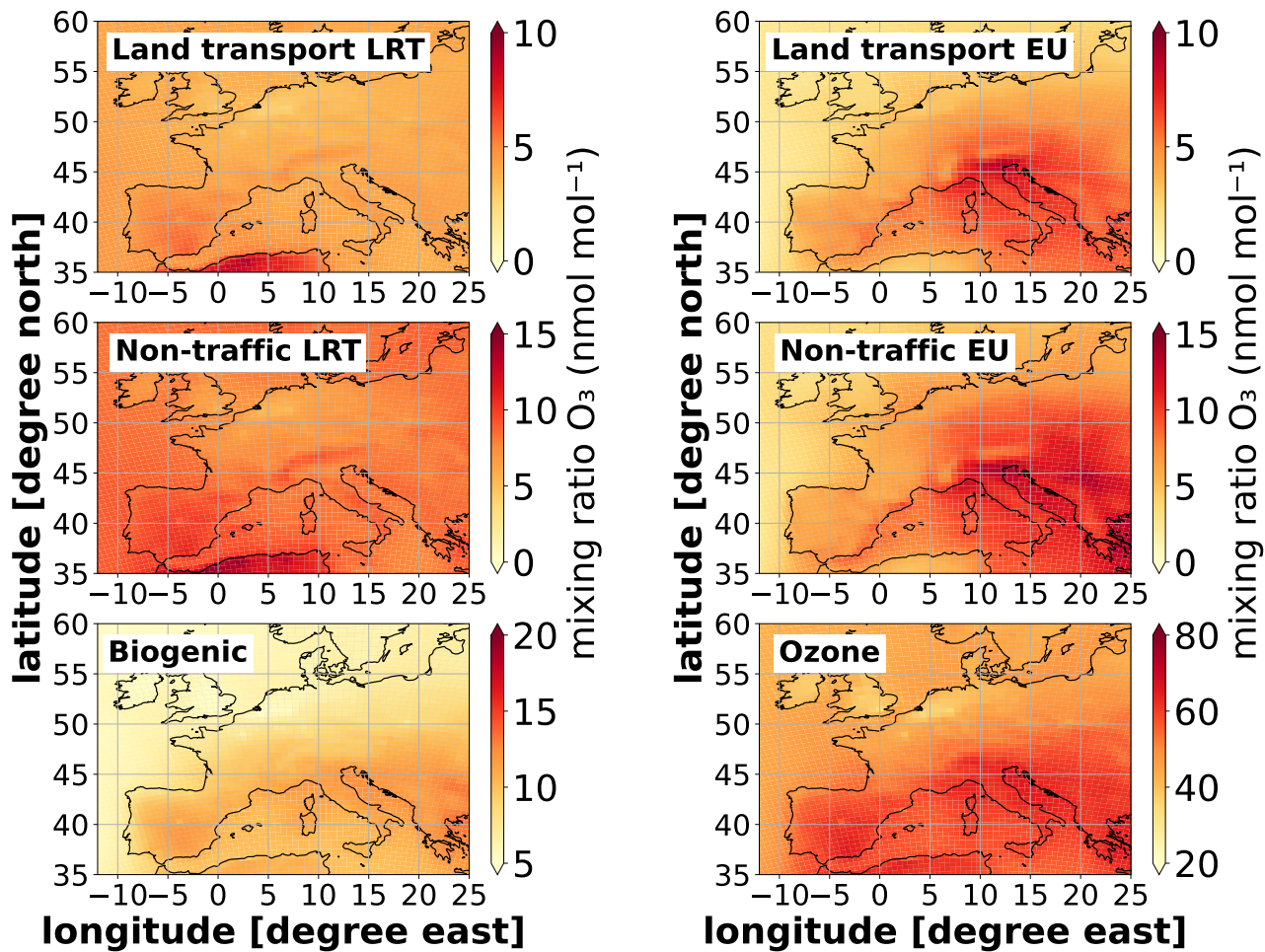


Figure S17. Monthly mean absolute contribution as mixing ratios in nmol mol^{-1} of O_3 for JJA 2017 from long-range transported (LRT: ROW + NA + EA), biogenic and European emissions as simulated with CM50.

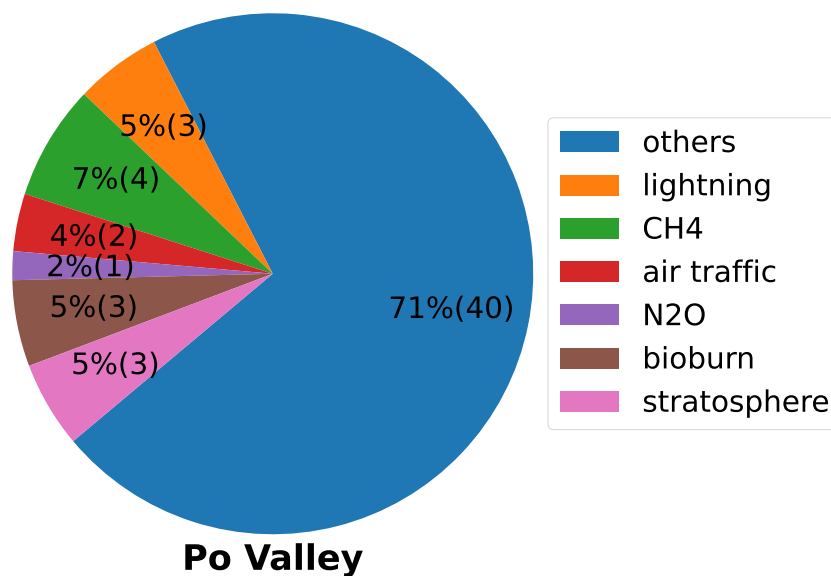


Figure S18. Absolute (brackets) and relative contribution as mixing ratios in nmol mol^{-1} and % of all sectors to ground-level O_3 as monthly mean for July 2017 in the Po Valley. Here, "Others" indicates the sum of the sectors land transport, anthropogenic non-traffic, shipping, and biogenic.

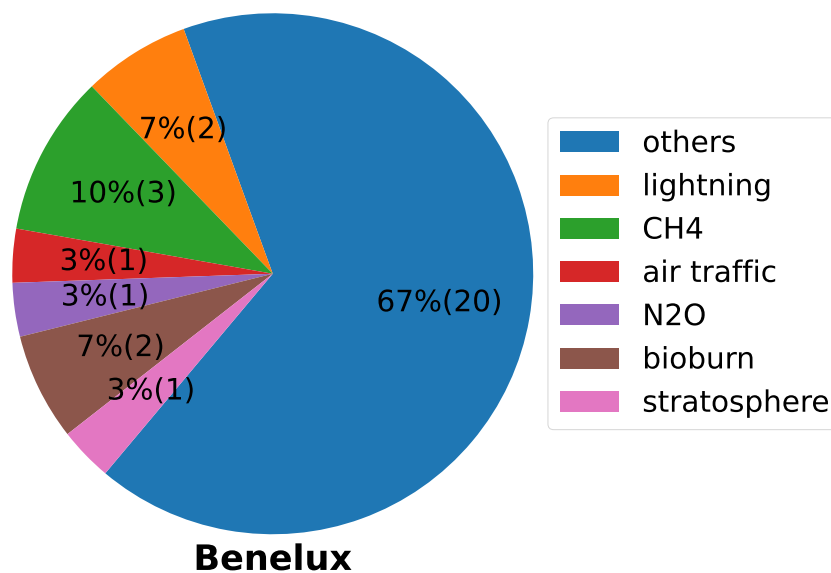


Figure S19. Absolute (brackets) and relative contribution as mixing ratios in nmol mol^{-1} and % of all sectors to ground-level O_3 as monthly mean for July 2017 in the Benelux region. Here, "others" indicates the sum of the sectors land transport, anthropogenic non-traffic, shipping, and biogenic.

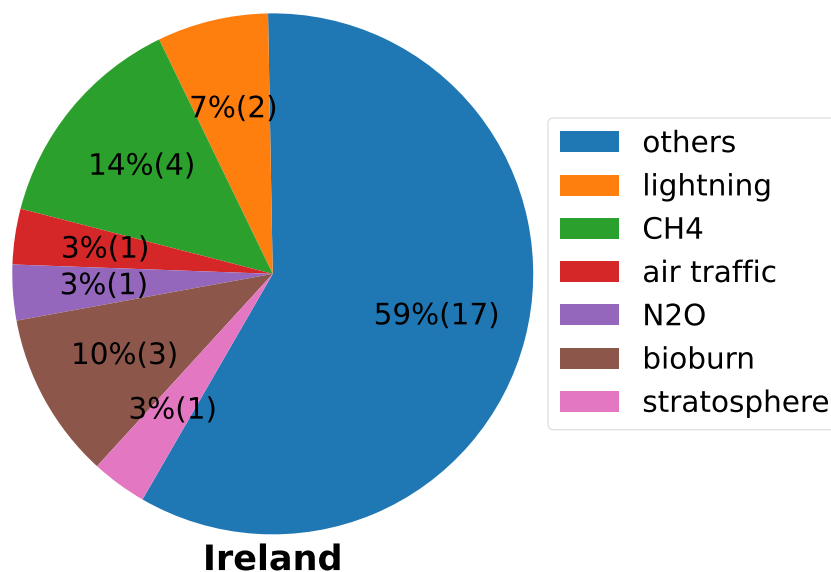


Figure S20. Absolute (brackets) and relative contribution as mixing ratios in nmol mol⁻¹ and % of all sectors to ground-level O₃ as monthly mean for July 2017 in Ireland. Here, "others" indicates the sum of the sectors land transport, anthropogenic non-traffic, shipping, and biogenic.

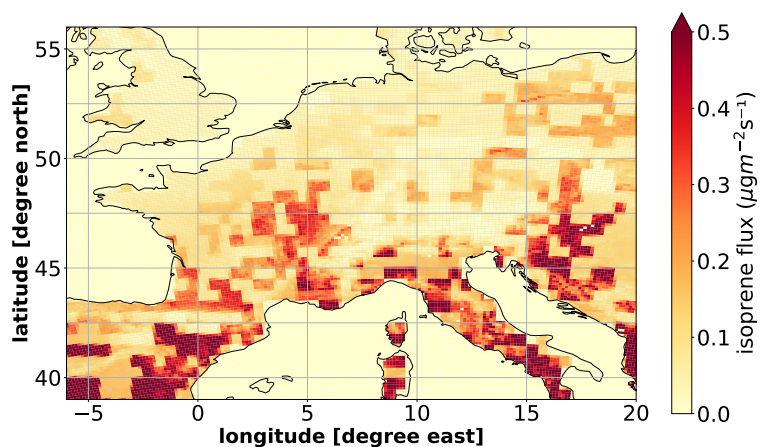


Figure S21. Mean of the ground-level isoprene (C₅H₈) emission flux in μg m⁻²s⁻¹ for JJA 2017 in CM12.

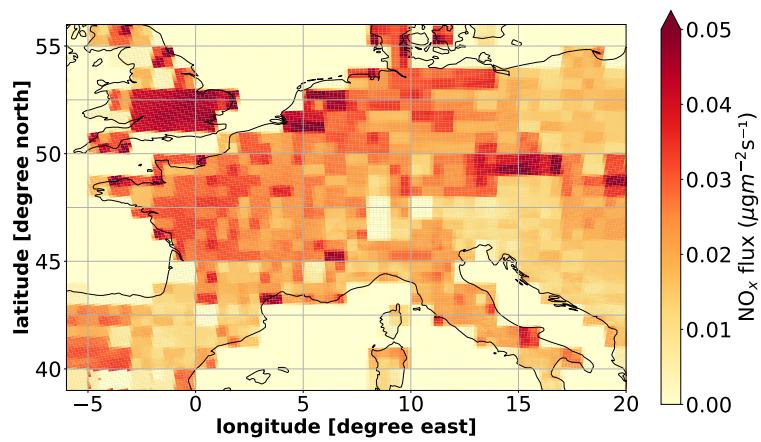


Figure S22. Mean of the ground-level soil NO_x emission flux in $\mu\text{g m}^{-2}\text{s}^{-1}$ for JJA 2017 in CM12.

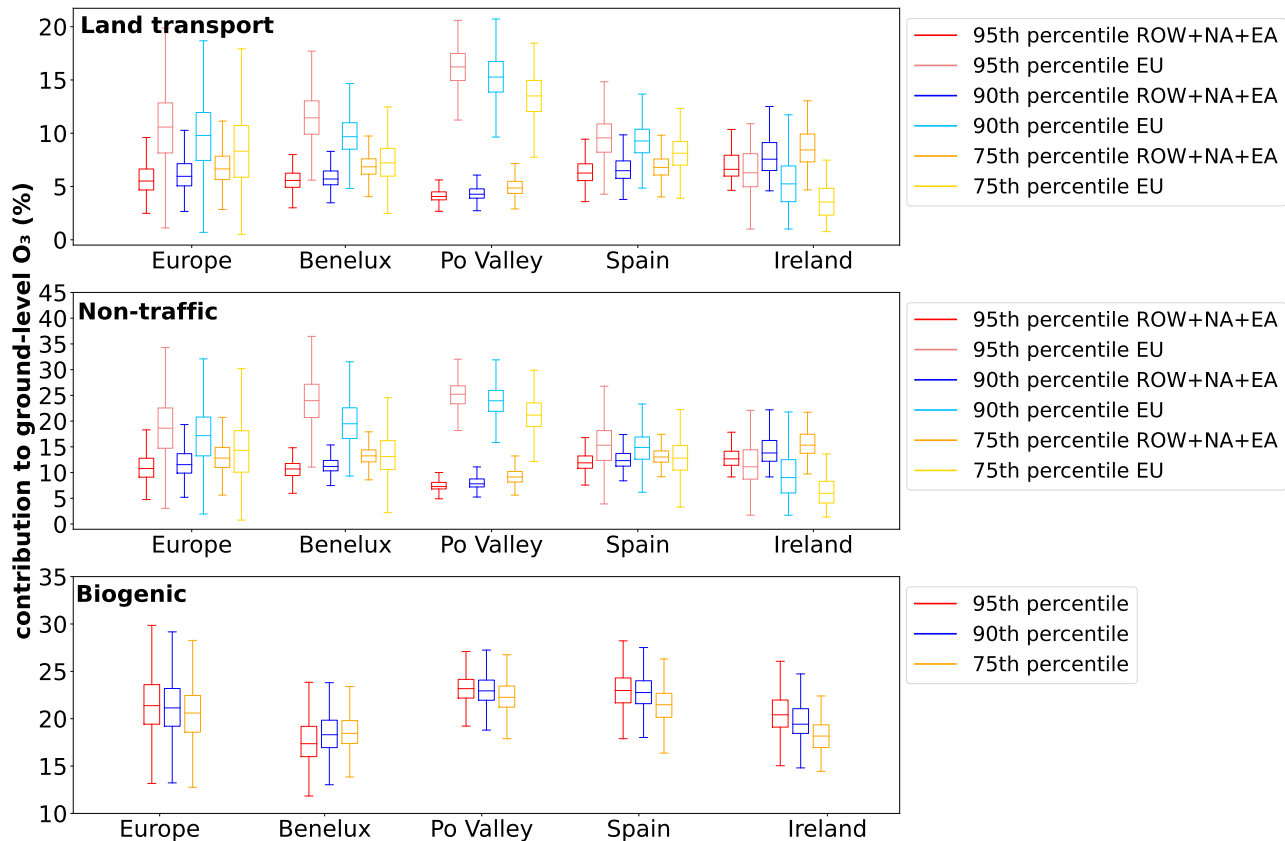


Figure S23. Box-whisker plot showing the monthly mean contributions of the most important emission sources at the 95th, 90th, and 75th percentiles of ozone as simulated by CM12 for July 2017. The first panel shows the relative contributions of O_3^{teu} and the sum of long-range transported relative contributions of O_3^{tra} , O_3^{tna} and O_3^{tea} . The second panel shows the relative contributions of O_3^{ieu} and the sum of long-range transported relative contributions of O_3^{ind} , O_3^{ina} and O_3^{iea} . The third panel shows the relative contributions of O_3^{soi} . The lower and upper ends of the boxes indicate the 25th and 75th percentile of the corresponding regional distribution, respectively, the bar the median, and the whiskers are defined as ± 1.5 the interquartile range of the contributions of all grid boxes within the indicated region.

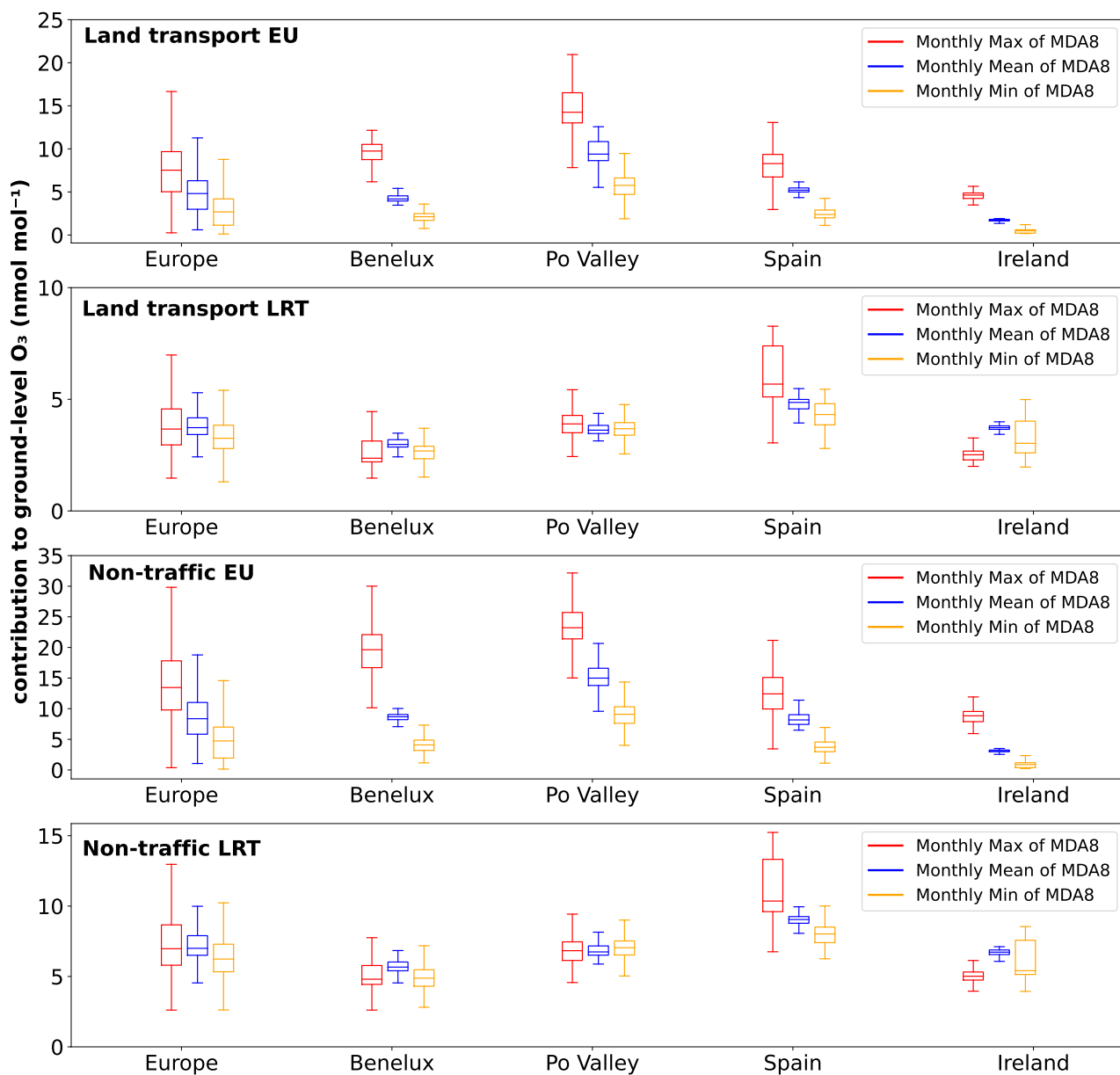


Figure S24. Box-whisker plot showing the contributions of the most important European emission sources of ozone as simulated by CM12 for July 2017. Shown are ozone contributions for European (EU) and long range transported (LRT) land transport and anthropogenic non-traffic emissions to ground-level ozone during the monthly maximum of the maximum daily 8-h average (MDA8), the monthly mean of MDA8 and the monthly minimum of MDA8 as ozone mixing ratio in nmol mol^{-1} based on 1-hourly model output. The lower and upper ends of the boxes indicate the 25th and 75th percentile corresponding regional distribution, respectively, the bar the median, and the whiskers the minimum and maximum contributions of all grid boxes within the indicated region.

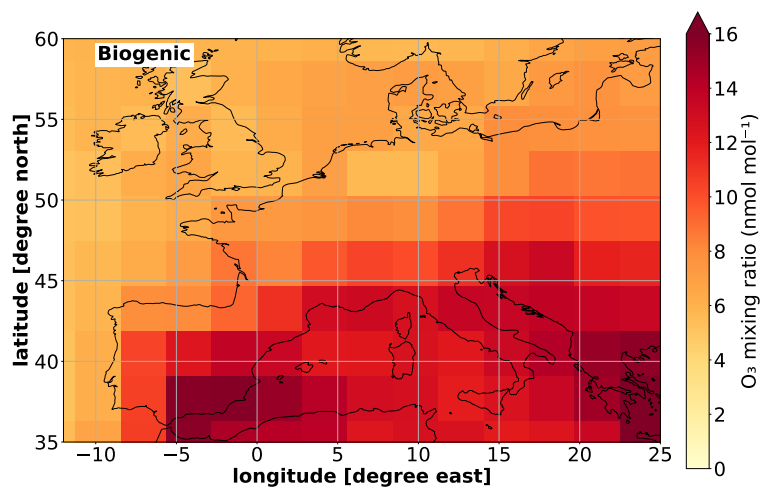


Figure S25. Mean absolute ozone contributions from biogenic emissions in July 2017 in EMAC.

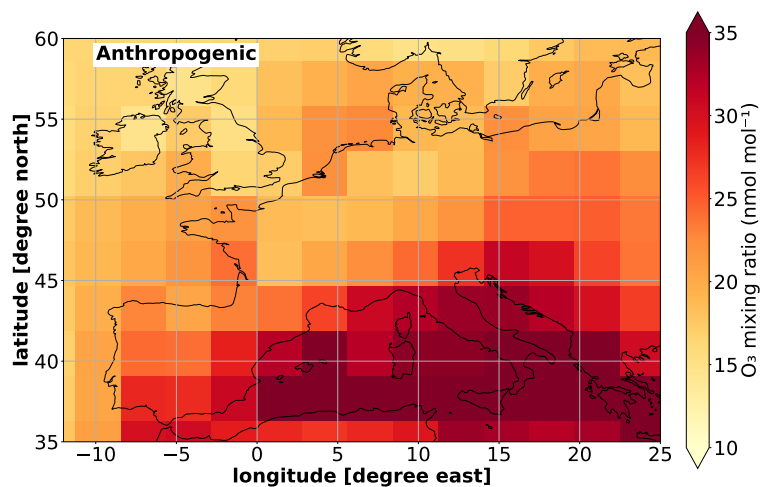


Figure S26. Mean absolute ozone contributions from anthropogenic emissions (land transport, non-traffic and shipping) in July 2017 in EMAC.

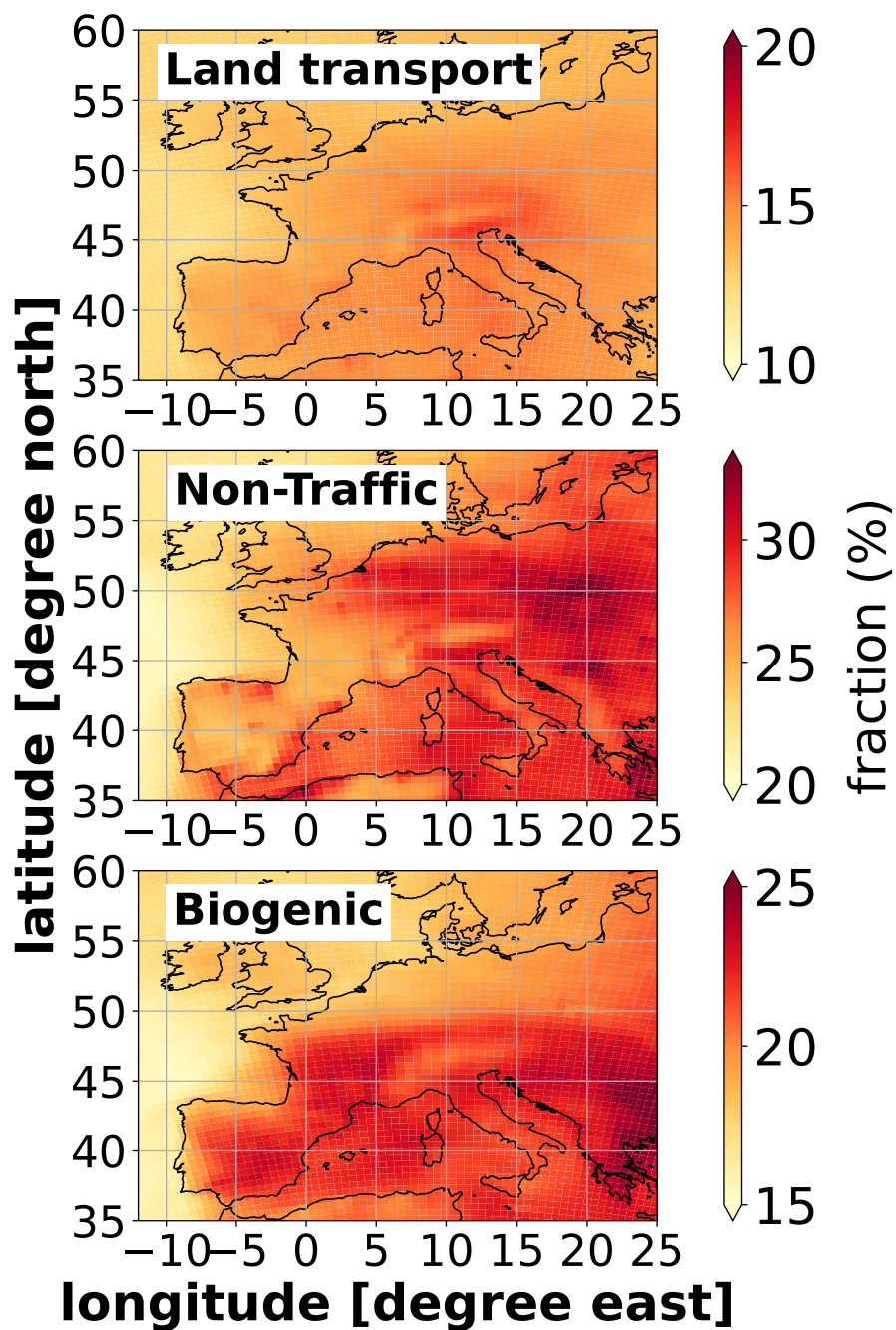


Figure S27. Monthly mean relative ozone contributions in % for JJA 2017 for the most important emission sectors as simulated with CM50.

References

- Johannes Bieser, A. Aulinger, Volker Matthias, M. Quante, and Hugo Denier van der Gon. Vertical emission profiles for Europe based on plume rise calculations. *Environmental Pollution (Barking, Essex : 1987)*, 159:2935–46, 05 2011. <https://doi.org/10.1016/j.envpol.2011.04.030>.
- 5 F. Dentener, J. Drevet, J. F. Lamarque, I. Bey, B. Eickhout, A. M. Fiore, D. Hauglustaine, L. W. Horowitz, M. Krol, U. C. Kulshrestha, M. Lawrence, C. Galy-Lacaux, S. Rast, D. Shindell, D. Stevenson, T. Van Noije, C. Atherton, N. Bell, D. Bergman, T. Butler, J. Cofala, B. Collins, R. Doherty, K. Ellingsen, J. Galloway, M. Gauss, V. Montanaro, J. F. Müller, G. Pitari, J. Rodriguez, M. Sanderson, F. Solomon, S. Strahan, M. Schultz, K. Sudo, S. Szopa, and O. Wild. Nitrogen and sulfur deposition on regional and global scales: A multi-model evaluation. *Glob. Biogeochem. Cycles*, 20:GB4003, 2006. <https://doi.org/10.1029/2005GB002672>.
- 10 V. Grewe, E. Tsati, M. Mertens, C. Frömming, and P. Jöckel. Contribution of emissions to concentrations: the tagging 1.0 submodel based on the modular earth submodel system (messy 2.52). *Geoscientific Model Development*, 10(7):2615–2633, 2017. <https://doi.org/10.5194/gmd-10-2615-2017>.
- Bastian Kern. *Chemical interaction between ocean and atmosphere*. PhD thesis, Johannes Gutenberg-University Mainz, 11 2013.
- S. Mailler, D. Khvorostyanov, and L. Menut. Impact of the vertical emission profiles on background gas-phase pollution simulated from the emep emissions over Europe. *Atmospheric Chemistry and Physics*, 13(12):5987–5998, 2013. <https://doi.org/10.5194/acp-13-5987-2013>.
- 15